Journal Pre-proof

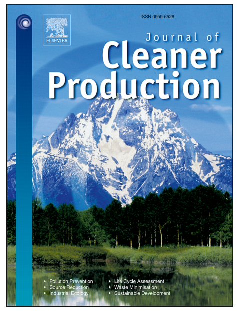

Effects of power tariffs and aeration dynamics on the expansion of water resource recovery facilities

Mani Firouzian, Michael K. Stenstrom, Diego Rosso

PII: S0959-6526(22)00031-2

DOI: https://doi.org/10.1016/j.jclepro.2022.130385

Reference: JCLP 130385

To appear in: *Journal of Cleaner Production*

Received Date: 19 July 2021

Revised Date: 22 December 2021

Accepted Date: 3 January 2022

Please cite this article as: Firouzian M, Stenstrom MK, Rosso D, Effects of power tariffs and aeration dynamics on the expansion of water resource recovery facilities, *Journal of Cleaner Production* (2022), doi: https://doi.org/10.1016/j.jclepro.2022.130385.

EFFECTS OF POWER TARIFFS AND AERATION DYNAMICS ON THE EXPANSION OF WATER RESOURCE RECOVERY FACILITIES

Mani Firouzian[1,*], Michael K. Stenstrom[2], Diego Rosso[1,3]

[1]*Department of Civil and Environmental Engineering, University of California, Irvine, CA, USA*

[2]*Department of Civil and Environmental Engineering, University of California, Los Angeles, CA, USA*

[3]*Water-Energy Nexus Center, University of California, Irvine, CA, USA*

(Corresponding author: e-mail: mfirouzi@uci.edu)

CRediT Authorship Contribution Statement

Mani Firouzian: Conceptualization; Data compilation; Data curation; Modelling; Formal analysis; Investigation; Methodology; Visualization; Writing original draft; Writing review & editing.

Michael K. Stenstrom: Experimental work; Writing review & editing.

Diego Rosso: Supervision; Conceptualization; Research design; Experimental work; Visualization; Writing review & editing.

EFFECTS OF POWER TARIFFS AND AERATION DYNAMICS ON THE EXPANSION OF WATER RESOURCE RECOVERY FACILITIES

Mani Firouzian[1,*], Michael K. Stenstrom[2], Diego Rosso[1,3]

[1]*Department of Civil and Environmental Engineering, University of California, Irvine, CA, USA*

[2]*Department of Civil and Environmental Engineering, University of California, Los Angeles, CA, USA*

[3]*Water-Energy Nexus Center, University of California, Irvine, CA, USA*

(Corresponding author: e-mail: mfirouzi@uci.edu)

Abstract

Water resource recovery facilities are major points of electricity demand and exhibit dynamic electricity demand due to their influent load as well as their diurnal and seasonal cycles. This dynamic demand along with the diurnal and seasonal nature of grid electricity cost as well as greenhouse gas emission intensity (i.e., emission produced to generate unit grid electricity) together demonstrate the importance of modelling these facilities dynamically to accurately assess their energy demand, operating cost, extent of removal, and greenhouse gas emissions. This article reports the results of a dynamic modelling effort that examines the effect of an expansion project on the extent of treatment, electricity demand, carbon footprint, and the operating cost of a large water resource recovery facility in California. This expansion consists of the addition of a differently configured activated sludge unit and associated secondary clarifiers to this plant's existing unit. The presence of these two parallel activated sludge configurations in the expanded plant was expected to provide an opportunity to achieve electricity demand and cost savings especially during the facility's coinciding peak of electricity demand with the grid's demand by maximizing the use of more energy efficient configurations. This electricity saving approach is an example of a grid demand-side flexibility project. However, the observed inverse correlation of the facility electricity demand and its cost with the overall operating cost and extent of treatment after the addition of the second activated configuration, which was determined to be the less energy efficient of these two configurations, demonstrated the infeasibility of such a grid demand-side flexibility project. This inverse correlation is changed to a positive correlation if the electricity efficiency of the added activated sludge configuration as part of this expansion project exceeds the existing electricity efficiency. As a result, recommendations were made accordingly for future studies to improve this configuration's electricity efficiency and to make the proposed grid demand-side flexibility project feasible. Such electricity efficiency improvement is also expected to lower the plant's overall carbon footprint which was not significantly impacted as part of this expansion project.

Key Words - Water Reclamation; Dynamic Modelling; Power Tariff; Duck-Curve; Greenhouse Gas Emissions; Dynamic Alpha Factor

Highlights

- Dynamic modelling is needed for a realistic analysis of wastewater treatment energy
- Realistic electricity cost estimation needs electricity tariffs and treatment dynamics
- Hourly alpha factor dynamics are responsible for treatment energy and cost variation

Graphical Abstract

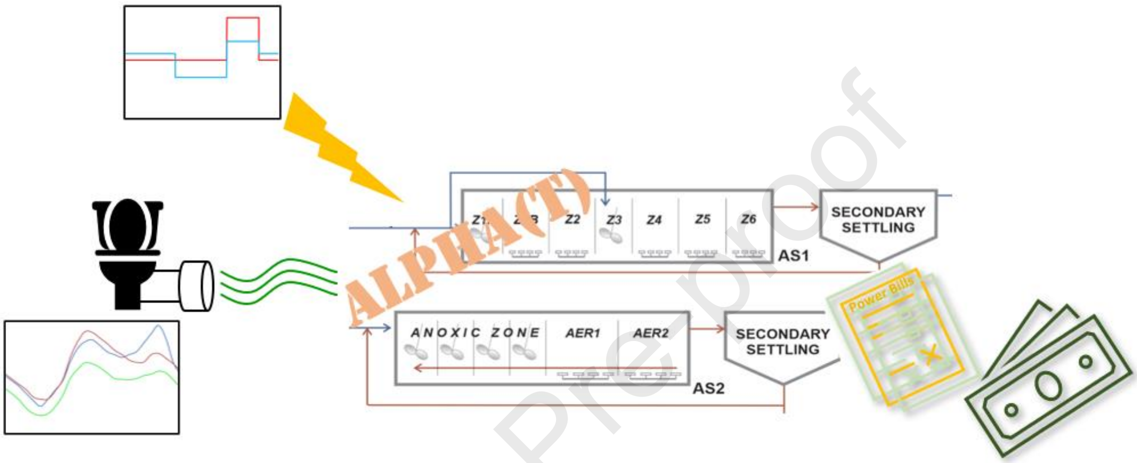

Abbreviations

AS: Activated Sludge
BOD: Biochemical Oxygen Demand
bCOD: Biodegradable Chemical Oxygen Demand
CAISO: California Independent System Operator
CBOD: Carbonaceous Biochemical Oxygen Demand
CEPT: Chemically Enhanced Primary Treatment
COD: Chemical Oxygen Demand
CSTR: Continuous Stirred Tank Reactor
DO: Dissolved Oxygen
EQI: Effluent Quality Index
GHG: Greenhouse gas
IQI: Influent Quality Index
L-E: Ludzack-Ettinger
MGD: Million Gallons per Day
MLE: Modified Ludzack-Ettinger
OTE: Oxygen Transfer Efficiency
QIR: Quality Index Removal
SCE: Southern California Edison Company
SOTE: Standard Oxygen Transfer Efficiency
TKN: Total Kjeldahl Nitrogen
TSS: Total Suspended Solids
WRRF: Water Resource Recovery Facilities

1 INTRODUCTION

Municipal water resource recovery facilities (WRRFs), formerly known as wastewater treatment plants, receive contaminants from sewers and are typically subject to diurnal cycles of loading. The daily dynamics of the influent to these facilities can exhibit ample variations which require flexible processes and equipment to perform the treatment necessary to meet discharge permits.

There are multiple constituents in wastewater usually quantified with aggregate definitions such as Biochemical Oxygen Demand (BOD) and Total Suspended Solids (TSS). BOD is a parameter widely used to determine organic pollution in both wastewater and surface water. This measurement of oxygen demand is an indirect measure of pollution in that it involves the measurement of dissolved oxygen that is consumed by microorganisms to biochemically oxidize the organic matters or pollutants in the water sample (Metcalf & Eddy, 2014). TSS is another important parameter used to quantify water pollution and is measured by passing the wastewater through filters with pore size varying from 0.45 to 2.0 µm and drying and weighing the solids captured by the filter (Baird, Eaton, Rice, & Bridgewater, 2017). Since the flowrate reaching the plant from the sewers and the concentration of the contaminants vary every hour of the day, the WRRF is inherently dynamic (Fig. 1).

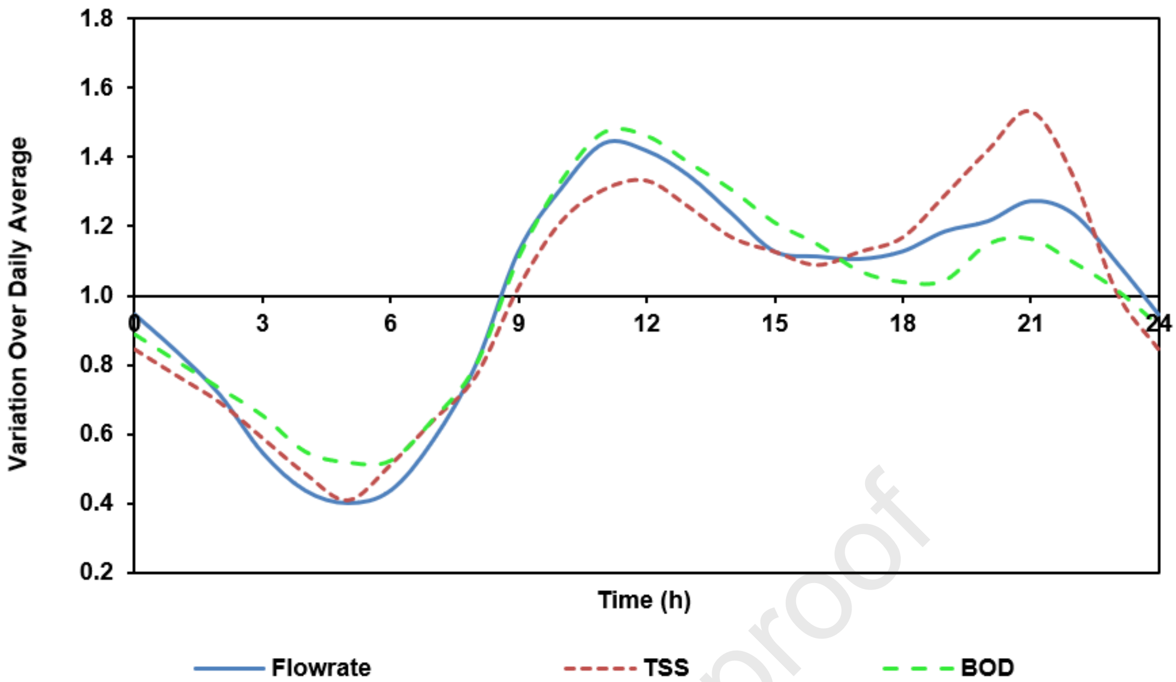

Fig. 1: Typical diurnal variations observed in flow, biological oxygen demand (BOD), and total suspended solids (TSS) in domestic wastewater normalized to their average hourly values (adapted from Metcalf & Eddy, 2014).

Although wastewater treatment is a minor energy consumer when compared to other components of the human energy footprint (Olsson, 2015), WRRFs require a significant amount of electricity to operate due to their substantially sized equipment and the large amount of wastewater that such equipment processes (Reardon, 1995). In a municipal setting, WRRFs are in the top tier of electricity demand facilities. Depending on having in-house electricity generation capabilities, WRRFs need to import a portion, or the entirety of their electricity needs from the electrical power grid (i.e., electricity gid, power grid, or the grid). Similar to WRRFs, power grids have diurnal cycles and typically their peak of electricity demand coincides with the peak of WRRFs' demands (Zohrabian et al., 2021).

Recent growth and the widespread use of photovoltaic electricity generation have been changing the diurnal trend of net electricity load (i.e., total load – photovoltaic) curves for the power grid, turning it into a duck-shaped curve (Howlader et al., 2017; Howlader et al. 2018). This change in the number and duration of the net diurnal electricity load peaks has changed the electricity tariff structure, and in many cases has resulted in a significant hike in its cost during the new peak of load (16:00-21:00). The main reason for this cost increase is the limited number of electricity generation sources that can respond to the short yet sharp ramp-up period prior to the new peak and their higher cost of operation (Gonzalez-Salazar et al., 2018; Howlader et al., 2018). Most of these electricity generation sources that are widely used rely on the combustion of fossil fuels (Howlader et al., 2018), which increases the carbon intensity of the grids' electricity (i.e., greenhouse gas emissions produced to generate unit grid electricity in kg CO_2eq kWh^{-1}) during these peak periods.

The large electricity consumption by WRRFs, the coinciding of their electricity demand peaks with the grid's, and the effect of the increase in variable-generating renewable sources (e.g., photovoltaic) on the grid's diurnal dynamics and cost (hence, WRRFs electricity cost) had made these facilities an attractive target for demand-side flexibility projects (Zohrabian et al., 2021). These projects consist of modifying the WRRF's operation to lower their electricity imports from the grid during the grid's peak of demand which usually results in lowering its electricity cost and carbon intensity. The demonstration of these flexibility projects' effectiveness at WRRFs requires experimental and simulation efforts (Zohrabian et al., 2021) that correctly capture the diurnal cycles or dynamic trends of these facilities as well as of the grid. As such, the dynamic grid electricity fee schedules and carbon intensity profiles need to be fed into these dynamic simulations or models, in addition to dynamic influent characteristics profiles, to correctly assess the effect of these projects on a WRRF's electricity imports. In addition to a WRRF's electricity demand, the impact of these projects on other aspects of treatment such as effluent quality and overall operating cost of the plant need to be reviewed to guarantee the practicality and feasibility of these proposed projects.

There are many published studies on the effects of a modification of a WRRF on its overall operating cost, carbon-footprint, and energy savings. However, these studies did not use dynamic influent trends and dynamic models (*inter alia*, Musabandesu and Loge, 2021). Even when dynamic modelling of the treatment process utilizing dynamic influent characteristics was performed, the cost or carbon intensity of the electricity imports from the electricity grid were assessed using average values as opposed to the diurnal variable ones (Gori et al., 2011; Gori et al., 2013). As such, none of these studies' results are realistic representations of the diurnal nature of these plants' operations, operating costs, and carbon footprints (Caliskaner et al., 2016; Caliskaner et al., 2017; Caliskaner et al., 2018; Pasini et al., 2020). Examples of studies that did not account for either dynamic electricity imports cost and carbon intensity or dynamic facility influent have been recently performed on the effect of primary treatment and the use of advanced primary treatment technologies on the operation of different WRRFs (Aymerich et al, 2015; Panepinto et al, 2016; Schäfer et al, 2017). Lack of dynamic influent, grid electricity cost, or carbon intensity profiles in these many modelling examples demonstrates the need for a true dynamic comprehensive model which Zohrabian et al. (2021) highlighted in their study.

In contrast to previous modelling examples provided, this study employs a completely dynamic simulation model that was developed using dynamic influent characteristic derived from the field data as well as the grid's dynamic electricity tariffs and carbon intensities profiles. The process modification focused on here consists of the plant's activated sludge process expansion by adding a different configuration to the existing one at a large WRRF in the state of California. Although this modification expanded the facility treatment capacity, the results of the dynamic models developed for pre- and post- modification scenarios can be fairly compared by normalizing them to the extent of treatment. Such a comparison demonstrates how combining these two different activated sludge configurations will impact the facility's overall electricity demand, carbon footprint, and operating cost. It also allows the indirect comparison of the newly added configuration with the existing one. This is the preliminary step to determine whether the addition of the new activated sludge technology can be qualified as a demand-side flexibility project. Hence, the goal of this paper is to determine whether the parallel use of these two activated sludge configurations in a facility would create electricity demand savings.

This goal is achieved by first assessing the effect of the addition of the second configuration on the electricity demand, overall operating cost, carbon footprint, and effluent quality of this facility which is the focus of this study. Depending on this study's findings, future detailed studies can be coordinated and performed on technicality and the extent of changing the influent distribution between these two activated sludge configurations as a demand-side flexibility project. This article also summarizes a few of the main challenges that were encountered when preparing the dynamic model used in this study. These challenges and how to cope with them can also be important topics for future studies or updates to improve this facility's existing standard operation procedures. Finally, this article provides a brief explanation of the limitations of expanding the results of this study to the other WRRFs, lists some of the factors that cause such limitations, and identifies areas where future research is needed to increase the modified or expanded plant's energy efficiency.

In addition to providing more realistic results, the dynamic model developed here can also pinpoint the time of the day or year when the plant's electricity demand, carbon footprint, or operating cost is higher. This allows the WRRFs' management to achieve considerable energy, cost, or carbon footprint reduction by focusing on optimization and demand-side flexibility projects targeting these periods which can result in lowering the capital cost of such projects compared to those that target the entire operating period.

2 METHODS

2.1 Current and Post-Expansion Plant Scenario

This study was performed on a large WRRF located in California that currently treats a peak influent flow of 5.30×10^5 m^3 d^{-1} (140 million gallons per day, or MGD). This facility is currently the main facility of a two-plant network treating on average a combined flow of 7.57×10^5 m^3 d^{-1} (200 MGD). More than half of this network's effluent is used for reuse purposes, specifically groundwater recharge and sea-water barrier intrusion, and the remainder is discharged to the Pacific Ocean.

Prior to pumping into the ground injection wells for reuse, the effluent of the WRRF studied here underwent treatment for reuse, at a neighbouring facility. As such, this plant's primary treatment goal is the removal of TSS and BOD to prepare the effluent for downstream microfiltration. Although nitrogen (i.e., ammonia, nitrate, and nitrite) removal is not a concern for this plant, it is practiced here to improve secondary solids separation and as an energy-savings measure (Rosso and Stenstrom, 2007).

The current plant utilizes chemically enhanced primary treatment (CEPT) using ferric chloride and anionic polymers for its primary treatment stage. On average, about 20% of the primary effluent is sent to the plant's two trickling filters equipped with one clarifier each. The remaining 80% of the primary effluent is split between Activated Sludge Unit #1 (AS1) and Activated Sludge Unit #2 (AS2) at a 40/60 ratio, respectively, on average. AS1 configuration is a step-feed Ludzack-Ettinger (L-E) while AS2 is a Modified Ludzack-Ettinger (MLE), and each has its own secondary clarifiers network. Fig. 2 illustrates the overall process configuration of the post-expansion or current plant.

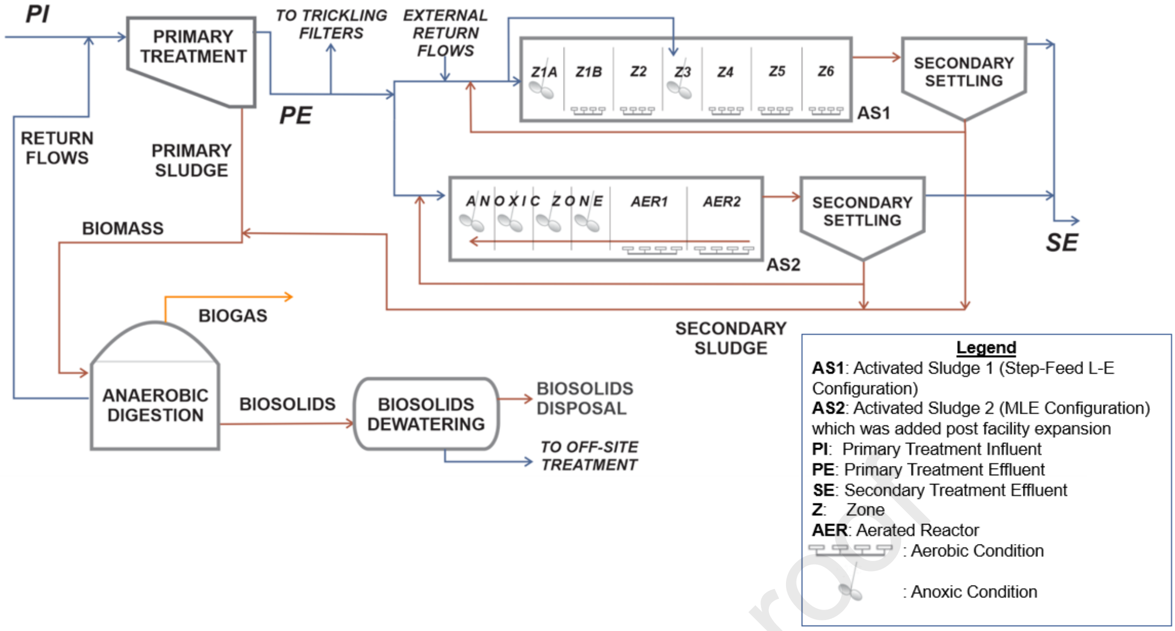

Fig. 2. Plant configuration after its expansion. Before the expansion, the plant was not equipped with AS2 and its secondary settling.

In the L-E configuration, the influent, which is the mix of primary treatment effluent and return sludge from secondary settling, is fed to an anoxic zone and then to aerobic zones. The nitrate in the return sludge from the secondary clarifiers is used as substrate by denitrifying microorganisms in the anoxic zone and is converted to nitrogen gas that is released to the ambient air. The MLE configuration is an improved version of the L-E process, obtained by adding internal recirculation to the biomass (see Fig. 2), thereby providing higher degrees of nitrification and denitrification by increasing the amount of nitrate sent to the anoxic zone and converted to nitrogen gas, which otherwise would be limited to the nitrate in the return sludge (Metcalf & Eddy, 2014).

The AS1 in this facility uses the L-E configuration in a step-feed layout where two L-E units are put in series. About 40% of this activated sludge unit's influent is sent to the anoxic zone of the upstream L-E unit and the remainder 60% is mixed with the effluent of the upstream L-E unit's in the downstream L-E's anoxic zone. This configuration improves the nitrogen removal of an individual L-E process as it delivers more nitrate to the anoxic zone of the downstream L-E unit. Depending on the internal recycle stream flow in the MLE and the flow distribution in the Step-Feed L-E configurations, these configurations can achieve total effluent nitrogen less than 10 mg l^{-1}. The step-feed L-E provides higher treatment capacity per tank volume compared to the MLE. However, the MLE process is expected to provide improved nitrogen removal without adding to the aeration electricity demand since the recirculating stream has already undergone BOD oxidation. The internal recirculation pumps have high flow, but very low head, hence their energy requirements are minor when compared to the aeration blowers.

The thickened sludge from primary and secondary treatment units of this plant is digested anaerobically. The produced biogas is used in the facility's cogeneration unit to generate electricity and steam for the plant's operations. The plant also imports natural gas and electricity to meet the remainder of its energy requirements. Natural gas supplements biogas for electricity generation especially during the summer months when grid electricity costs are higher.

A small portion of AS1 effluent is used to support the treatment operations for this plant and its neighbouring advanced treatment plant (including cogeneration system cooling and microfiltration backwash in the adjacent reuse facility). Therefore, the effluents of these processes are returned to AS1 for treatment. The presence of nitrate in AS1 effluent which is recycled back to this process unit through these return streams promotes the nitrogen removal of AS1 (as explained above in the definition of the MLE process in this section). As such, the presence of these return streams in the facility AS1 slightly deviates the operation of AS1 from an only L-E to a *de facto* Hybrid L-E/MLE.

2.2 Old Plant, Step-Feed and Pre-expansion Scenario

The pre-expansion, old, or old step-feed plant scenario in this study can simply be described as the post-expansion plant without the AS2 or MLE activated sludge configuration. In other words, the expansion project added AS2 (i.e., MLE configuration) to the pre-expansion plant's existing activated sludge unit (i.e., AS1) which utilized step-feed L-E configuration. Prior to the plant expansion, the entire primary effluent minus the constant portion that was sent to the trickling filters would be treated in the AS1 or step-feed L-E process. Without the AS2, the pre-expansion facility had lower treatment capacity. The plant's peak influent flow prior to the expansion was about 3.79×10^5 m^3 d^{-1}

(100 MGD) and the two-plant network treated on average a combined flow of 7.57×10^{5} m^{3} d^{-1} (200 MGD).

2.3 Modelling Tool and Protocol

To perform dynamic modelling, BioWin 6.1 (EnviroSim; Hamilton, ON) was utilized using the Good Modelling Practice Protocol (Rieger et al., 2013). The monthly average process data from the plant was used for calibration and validation. Specifically, October through December 2018 monthly data were used for calibration, and January through September 2019 data was used for validation. Dynamic hourly influent profiles were derived from these monthly averages as explained in more detail in the Data Collection section of this article. Default values in the simulation software (EnviroSim, 2020) were used here unless otherwise described.

In addition to modelling the treatment processes, electricity demand was also quantified for main equipment units (e.g., pumps and blowers). The additional electricity demand for the unit operations not available in the process simulation software (ex. minor process pumping, odour control, process control equipment, etc.) was calculated by subtracting the electricity demand of the calibrated model from the total electricity demand from the field data and so was accounted for in the simulation. The supplemental natural gas used for electricity generation was also accounted for. The plant blowers, plus the cogeneration electricity and thermal energy efficiencies, were also calibrated using field data.

The trickling filters were excluded from the dynamic model to increase computational efficiency because they received a constant aliquot of primary effluent, with the dynamic portion of the flow going to the activated sludge units. However, the trickling filters' electricity demand was entered into the model to estimate its contribution to the plant's total electricity demand. The effluent of the trickling filters is mixed with the effluent of AS1 and AS2 effluents before being sent to the neighbouring facility for further treatment. The effluent characteristics of the trickling filters were assumed to be the same as for the activated sludge units for this study.

Each of the plant's treatment processes consist of multiple identical units (e.g., AS basins, clarifiers). The total count and the count of the in-service equipment are summarized in Appendix B. Simulating all of these active, identical, and repetitive equipment slows down the simulation. It is common practice to simplify the modelling by treating the plant as the single smallest functional unit that could be scaled back to the plant total by means of a constant multiplication. Thus, the entire plant was divided into 6 identical trains and only one of these was simulated, accounting for one sixth of the plant influent flow to optimize the simulation's run time. This is a usual practice for efficient modelling of processes with redundancies such as WRRFs. The number of trains selected here is the smallest set of identical process units that this plant can be reduced to. The results of the single-line simulations were subsequently scaled up to the total by multiplying the results times the total number of trains.

2.4 Data Collection

2.4.1 Influent and Temperature Profiles

To perform the dynamic simulation, hourly influent profiles including at least flow, chemical oxygen demand (COD), and total Kjeldahl nitrogen (TKN) concentration are required. Similarly to BOD, COD is a quantification of the water pollutants consuming oxygen. However, in COD tests the material is oxidized chemically using dichromate in an acid solution which does not distinguish between biodegradable and non-biodegradable material (Metcalf & Eddy, 2014). COD is a desirable variable for process modelling because it includes the constituents that are not biodegraded but could be settled or removed otherwise. TKN is another typical parameter used for measuring water pollution through the Kjeldahl method and it represents the aggregate of ammonia and total organic nitrogen (Metcalf & Eddy, 2014).

The post-expansion plant data collection system records only monthly averages. However, the plant hourly influent flow data was available for one month immediately preceding the study period here. This hourly flow data was used to calculate an average daily flow and then average instantaneous (hourly) to average daily flowrate ratio (or hourly flow factors) for each hour of the day. For each hour of the day, for all days of the month when data was available, the average and standard deviation of hourly flow factors were calculated (refer Fig. A.1 in Appendix A). These average instantaneous factors were then applied to each average monthly influent entity to prepare hourly profiles for each hour of the day in that month upon consulting and confirming with the plant personnel due to the lack of hourly concentration data.

Fig.3 illustrates the hourly influent flow and concentration profiles derived here for the twelve-month study period. These hourly profiles were also used in the simulation to perform the final calibration of the model after calibrating it with monthly averages. In the absence of COD data sets, the typical Carbonaceous BOD (CBOD) to COD ratio (0.38) provided by the plant was used to reconstruct COD data from CBOD field measurements. CBOD is the measure of oxygen demand employed for oxidizing the oxidizable carbon in the wastewater sample with an inhibitor of nitrification (Metcalf & Eddy, 2014).

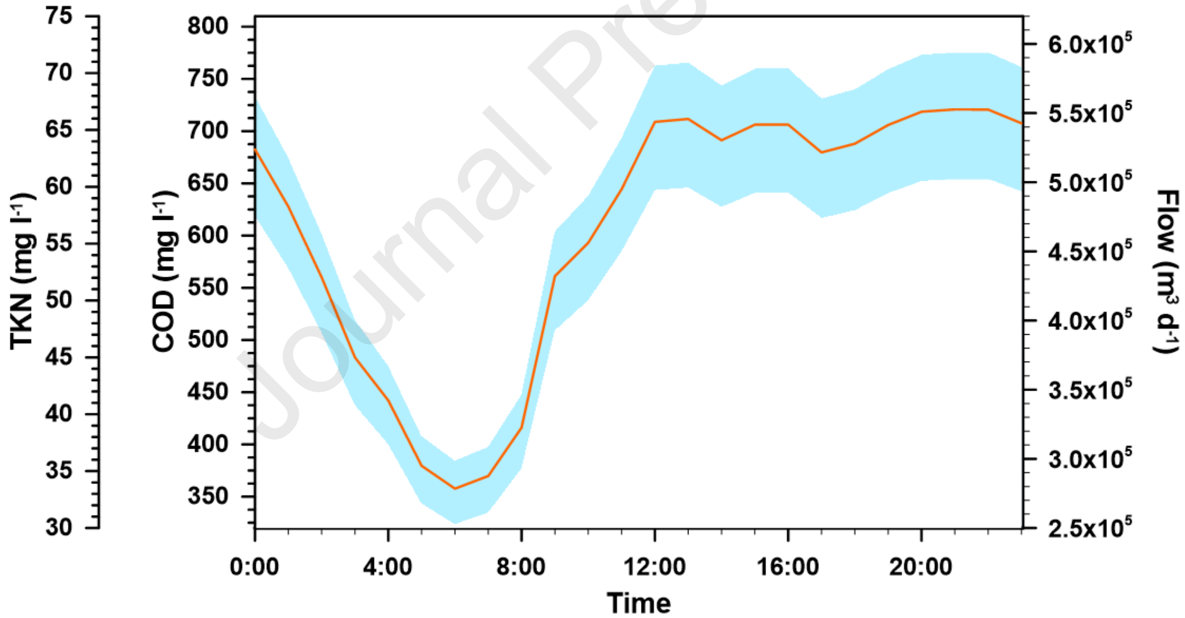

Fig. 3. Post-expansion plant influent dynamic trends for October 2018 through September 2019 derived from monthly averages and multiplied by an hourly flow factor based on the ratio of instantaneous to average monthly flows. All three Y-axis apply to the data points plotted. Shaded in blue is the range of the entities shown on each Y-axis during this 12-month period and the red line represents their hourly averages over one year.

The post-expansion plant influent dynamic trends in Fig.3 were used to model this scenario. To model the pre-expansion scenario, the dynamic flow trend in Fig. 3 was adjusted to account for the lower treatment capacity and influent flow of this scenario (74.97% of the current). The pre-expansion plant average influent flow rate was back-calculated from the average activated sludge process' total influent flow and hydraulic retention time (HRT) data collected during a field-testing campaign at this plant with the goal of measuring its AS' oxygen transfer efficiency (explained in detail in the next section) in process conditions. In this back-calculation, the trickling filters' average influent flow at the pre-expansion plant was assumed to be the same as the post-expansion's.

Temperature effects on process physical-chemical and biokinetics constants are well documented and temperature-based calibrations have been extensively used in the past (Rieger et al., 2013). Hence, we incorporated the temperature dynamics in addition to the dynamic influent concentrations by using average daily ambient temperature data for October 2018 through September 2019 from the weather station closest to this plant (Weather Underground, 2021). The wastewater temperature in this collection area spans between minimum and maximum temperatures of 20°C and 30°C, occurring in March and September, respectively based on wastewater temperature trends from neighbouring facilities. Hence, we varied the temperature over the yearly cycle using a sinusoid with a 12-month period, average of 25ºC, amplitude determined by the temperature variation, and peak on the nineth month of the year in the absence of field wastewater temperature data for this facility.

2.4.2 Oxygen Transfer Efficiency and Alpha Factors

A field-testing campaign was carried out to measure *in situ* the oxygen transfer efficiency in process conditions (OTE, %). The OTE is the ratio of mass of oxygen transferred to the water over the mass of oxygen fed to the water through the compressed air line. In practical terms, the OTE represents the efficiency of the aeration process. We measured OTE using the off-gas method following the American Society of Civil Engineers (ASCE) testing protocol (American Society of Civil Engineers, 2018). The measurements of water temperature and dissolved oxygen (DO) were used to correct OTE to standard conditions in wastewater ($\alpha \times$ SOTE, %). Using oxygen transfer efficiency data in clean water from the air diffusers' manufacturer, we calculated *a posteriori* the α factor (i.e., the ratio of the oxygen transfer rate in process water to that in clean water, used for calculating aeration electricity demand), which represents the effects of wastewater pollutants on oxygen transfer efficiency (USEPA, 1989).

To model the activated sludge basins dynamically, a dynamic alpha trend for each aerated basin was needed. Although the simulation software used here did not provide for a dynamic alpha, it allowed the user to enter a time-dependent alpha diurnal schedule for each aerated reactor. The result of off-gas testing on AS1 was used for modelling the AS1 for both scenarios. Since no alpha data was available for AS2 in the post-expansion plant, the alpha values of AS2 were estimated matching the calculated DO concentrations with field data during the calibration period. The alpha values used for the simulation of AS1 and AS2 are presented in Table 1.

Table 1. Ranges of alpha factors used to describe the aeration dynamics in the activated sludge reactors. The alpha factor is not defined for anoxic zones.

Pre- and Post-Expansion Scenarios (Activated Sludge 1)

Zone:	Zone 1A	Zone 1B	Zone 2	Zone 3	Zone 4	Zone 5	Zone 6
Max	Anoxic	0.66	0.79	Anoxic	0.91	0.94	0.75
Min	Anoxic	0.37	0.66	Anoxic	0.55	0.62	0.65
Average	**N/D**	**0.48**	**0.74**	**N/D**	**0.69**	**0.83**	**0.71**

Post-Expansion (Activated Sludge 2)

Zone:	Anoxic Zone	Aerobic Zone 1	Aerobic Zone 2
Max	Anoxic	0.59	0.82
Min	Anoxic	0.33	0.50
Average	**N/D**	**0.43**	**0.62**

Dynamic hourly trends for alpha were derived using the dynamic alpha equation from Jiang, Garrido-Baserba et al. (2017) for each aeration basin, where alpha is a function of the applied COD. These calculated hourly ratios were then applied to the average alpha factors in Table 1 (details in Fig. C.1 in Appendix C).

2.4.3 Energy and Emissions Data

The natural gas caloric value was derived from the default high heat value in the greenhouse gas (GHG) combustion emission calculation protocol by the U.S. EPA, which is also used for GHG emission calculations in this study (U.S. EPA, 2016). The employed process units' electricity demand ratings as well as other parameters used to estimate electricity demand are listed in Appendix B. To determine the GHG emissions associated with the electricity imported from the grid, the dynamic hourly average carbon intensity for the grid's electricity was calculated from the data obtained from the California Independent System Operators (CAISO; California Independent System Operator, 2021) for each month of the year (details in Appendix D).

In addition to electricity importation (indirect GHG emissions), we calculated: the direct GHG emissions associated with combustion of biogas and natural gas; CO_2, N_2O, and CH_4 emissions associated with activated sludge biological treatment; CO_2 emission associated with sludge digestion; and CH_4 from biogas fugitive leaks. Fugitive methane emission associated with biogas leak was assumed to be 1% of the total methane generation in the digesters. The total GHG emission was then reported in CO_2eq units by multiplying each mass flow times their respective global warming potential.

2.4.4 Operating Cost

The costs of chemicals used for the treatment were calculated using the software defaults (EnviroSim, 2020) except for the anionic polymers used for CEPT whose cost (32.13 USD per 1000 m^3 of primary treatment influent) was obtained from the chemical provider (NSF Polydyne Inc.; Riceboro, GA). The cost of ferric chloride and anionic polymers used for primary treatment enhancement as well as chemical additives used in sludge dewatering and thickening processes were accounted for in this study. For sludge disposal cost calculations, also accounted for in this study, the simulation software default cost option for dry sludge disposal (cost per unit mass of TSS) was used (EnviroSim, 2020). Natural gas imports cost was also accounted for using the software default price factor (EnviroSim, 2020).

The cost of electricity imported from the grid was calculated using Southern California Edison's (SCE's) Time-of-Use tariffs presented in Schedules TOU-8-S and TOU-8-RTP-S (Southern California Edison, 2021). These price schedules are for facilities with a electricity demand higher than

500 kW, capable of generating electricity in-house, and determined to be the most representative tariffs for this WRRF compared to other price schedules available on SCE's website at the time of this study. Metering, energy usage (delivery and generation), and fixed and time related demand charges from these tariff schedules were used to calculate the cost of imported electricity for the two scenarios discussed here. Other charges such as voltage discount and power factors adjustment were not used as they were not applicable or the necessary data for calculating them (i.e., kVAR) could not be generated in this modelling effort.

TOU-8-RTP-S provides real time hourly pricing for the energy usage charges, while TOU-8-S offers constant pricing for each time-of-use periods (e.g., on-peak, off-peak, mid-peak, etc). These fee schedules also offer different pricing based on the voltage at which the electricity is delivered (i.e., below 2kV, from 2kV to 50 kV, and above 50 kV). The average of the pricing for 2kV to 50 kV and above 50 kV for each charge category was used as a hybrid cost to simplify the electricity cost calculation yet address the more dominant and different delivered voltages at a typical large WRRF. In addition, only one meter charge was accounted for in the cost calculation.

Fig. 4 compares the total energy usage charges for a hybrid of 2kV to 50 kV and above 50 kV voltage categories for each of the tariffs listed in these two fee schedules for summer (June through September) and winter (non-summer) months. Comparing these tariffs' energy charges in Fig. 4 with the plant dynamic influent profiles in Fig. 3 clearly demonstrates the coincidence of the peak of the plant influent diurnal trends and the peak of the electricity grid dynamic usage charges for all of these selected tariffs. In addition, a comparison of the legacy (old) tariffs with the new ones (illustrated in Fig.4) also demonstrates how the new diurnal cost and peak periods have evolved, showing an increase in the electricity cost and a shifting or compressing of the peak period to 16:00 to 21:00 as explained in the Introduction section of this article.

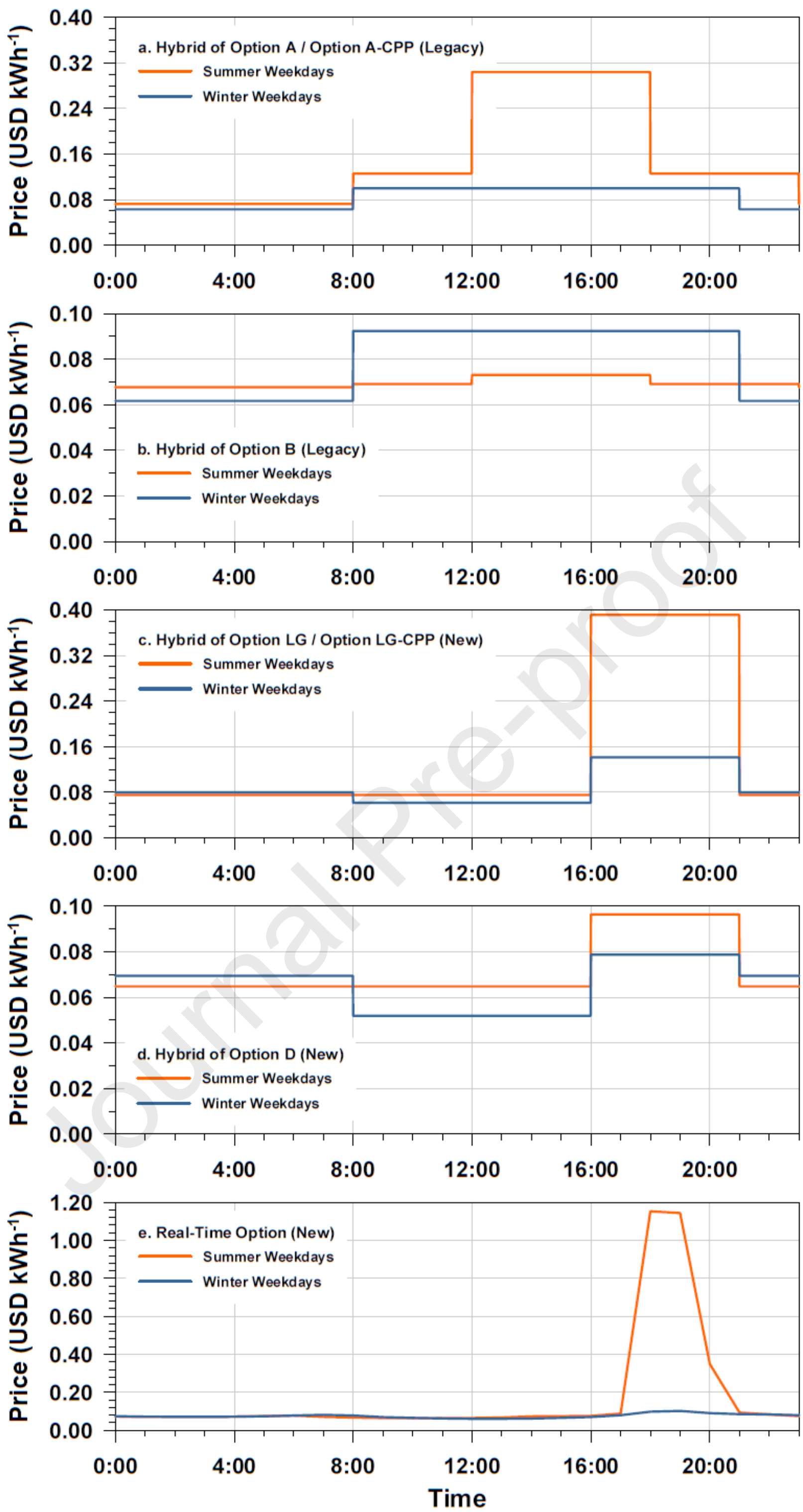

Fig. 4. Southern California Edison's tariff structures. **(a) to (d):** new and old (legacy) time-of-use schedule for total energy use charges for facilities with internal generation capacity and with the demand larger than 500kW (TOU-8-S) for weekdays derived from the average of fees scheduled for 2-50kV and >50kV grids [Effective as of March 1, 2019]. **(e):** current real-time schedule for total energy use charges for facilities with internal generation capacity and with the demand larger than 500kW (TOU-8-RTP-S) for weekdays derived from the average of fees scheduled for 2-50 kV and >50kV grids [Effective as of March 1, 2019] (Southern California Edison, 2021)**.**

The hybrid metering and demand charges that were calculated by averaging the charges for 2kV to 50 kV and above 50 kV categories are provided in Appendix J (Southern California Edison, 2021). Also, the standby demand of this facility used for demand charge calculations was assumed to be 5.2 MW (i.e., typical average inhouse generation capacity) per consultation with plant engineers.

2.5 Normalization of Results

To fairly compare these two scenarios' modelling for electricity demand, GHG emissions, and operating cost, these results are normalized to different parameters representing the extent of treatment. These normalization methods are as follows.

2.5.1 Normalization per Unit Influent Flow

The facility influent flow treated was used to normalize the model results for comparing the effluent quality and the net and total electricity demands of these two scenarios where net electricity demand is calculated by subtracting the facility in-house electricity generation from the total electricity demand. The normalized net and total electricity demands per unit influent flow are referred to here as net and total electrical energy intensities.

2.5.2 Normalization per Unit Activated Sludge Theoretical Oxygen Requirement

Theoretical oxygen requirements, defined as the amount of oxygen required for the removal of carbonaceous material and oxidation of ammonia and nitrite to nitrate, were used to normalize the electricity demand for comparing the activated sludge units of the two scenarios here. This normalized electricity demand is referred to as activated sludge energy intensity.

2.5.3 Normalization per Unit Quality Index Removal

The cumulative extent of the removal of all pollutants from wastewater for each scenario has been accounted for normalizing the net and total electricity demand, GHG emissions, and operating cost of each scenario to the plant's quality index (Jeppsson, et al., 2007; Nopens, et al., 2010) removal. Quality index removal (QIR) is defined as the difference between the weighted sum of TSS, TKN, COD, Nitrate, and BOD in the facility influent and effluent (more details in Appendix G).

2.5.4 Normalization per Unit Oxidized Load

Another approach used to compare the net electricity demand of these two scenarios is to normalize the net electricity demand to oxidized load or load removed defined as biodegradable COD (bCOD) load and nitrogen removed by oxidation. The bCOD represents the portion of the COD that can be biochemically oxidized. In calculating the oxidized load, the oxygen associated with oxidation of bCOD by denitrifying bacteria in the denitrification process (i.e., denitrification credit) needs to be subtracted if no supplemental carbon (e.g., methanol) is added to support the denitrification. The plant studied here does not add any supplemental carbon; therefore, this adjustment needs to be implemented to distinguish the actual oxidized load from the theoretical oxygen requirements (§2.5.2).

3 RESULTS AND DISCUSSION

Using the set of results generated in this project, we highlight the importance of overlaying process and energy dynamics to accurately assess the environmental impact of wastewater treatment facilities and to predict their real-time operating costs. Moreover, when life-cycle cost analyses are performed, the dynamics of operating costs become a necessary element for realistic cost projections (Amerlinck et al, 2016). Using the dynamic model in this study which accounts for both process and energy dynamics, we determined whether the addition of the new activated sludge configuration would allow the facility to define a new demand-side flexibility project. This proposed project would rely on changing the influent flow distribution between the plant's newly added and existing activated sludge configurations to maximize the energy savings of the configuration that is more energy efficient. For this assessment, the electricity demand, GHG emissions, and operating cost of the pre-and post-expansion scenarios are compared in this section. This comparison illustrates whether the addition of the new activated sludge configuration has improved the plant's electricity demand efficiency without increasing its overall operating cost, GHG emissions, and water pollution discharged which are key elements to justify this expansion as the starting point of a demand-side flexibility project.

3.1 Effluent Quality

Comparing the effluent constituents for the pre- and post- expansion scenarios showed lower ammonia and CBOD and comparable nitrate and TSS concentrations in the post-expansion plant. A more detailed comparison of these effluent dynamic trends is provided in Appendix F. To simplify the comparison of effluent quality for these scenarios, a cumulative comparison was conducted using the effluent quality index (EQI) (Jeppsson, et al., 2007; Nopens, et al., 2010). Note that EQI is a weighted measure of pollution, hence higher EQI is opposite to effluent quality (see Appendix G for details). Since the post-expansion scenario treats higher influent flow compared to pre-expansion, the EQI values were normalized to the plant total influent flow for this comparison. Comparing the monthly EQI for these two scenarios demonstrates that the post-expansion plant's index is lower by 3 to 6% from June through December, slightly higher in January and May (1.2 to 1.5 % respectively), and higher by 6 to 12% in February through April when compared to the pre-expansion's index. The facility received a significant amount of rain in February through March which may have contributed to the significant discrepancy between the overall EQI trend observed for these months compared to the other months. As such, the expanded plant delivers the same or better quality of treatment compared to pre-expansion scenario.

3.2 Electricity Demand Dynamic Trends and Annual Breakdowns

Dynamic net and total electrical energy intensities (i.e., electricity demand divided by influent flow) for both scenarios are shown in Fig. 5. This figure illustrates that the overall improved effluent quality after expansion corresponds to an increase of up to 0.07 kWh m^{-3} in total electrical energy intensity when compared to the pre-expansion scenario. Almost the same range of increase (0.02 to 0.10 kWh m^{-3}) is observed in the net electrical energy intensity which accounts for the plant's internal electricity generation.

The total electrical energy intensity is minimum or close to it at the peak of plant influent load (between 12:00 and 23:00) while the net intensity is maximum. This is despite the fact that the hourly trends for both the net and total electricity demands follow the same trend as influent flows and net electricity demand energy intensities and all peak between 12:00 and 23:00. As such, the reciprocal trend of total and net electrical energy intensity in Fig. 5 is due to a different magnitude of the net and total electricity demand values compared to influent flows where these demand values are normalized to the same influent flows to calculate the net and total energy intensity values here.

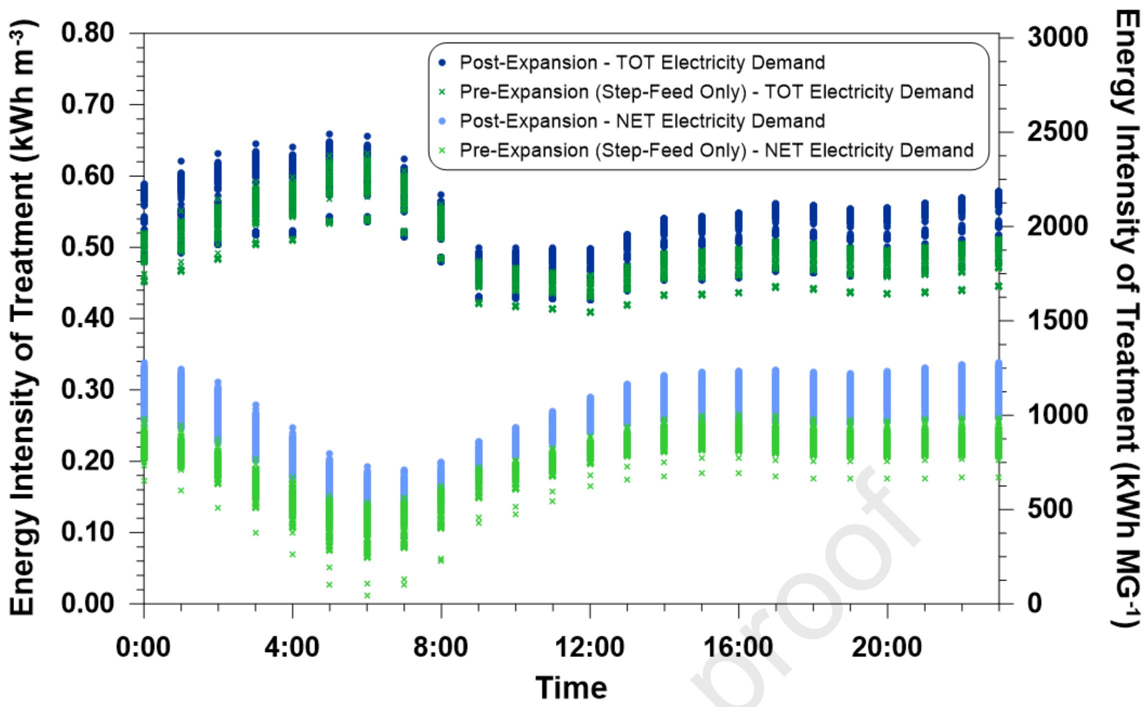

Fig. 5. Dynamic net and total treatment electrical energy intensities (demand normalized to plant influent flow) for the pre- and post-expansion scenarios. Both Y-axis apply to the data points plotted.

Finally, comparing the dynamic net electricity intensity trends in Fig. 5 with the grid's electricity tariffs and GHG emission intensity diurnal trends in Fig. 4 and Fig. D.1 in Appendix D, respectively, illustrates the coincidence of the peak of these three parameters for both scenarios at this WRRF. The coinciding of these peaks is similar to the references mentioned in the Introduction section. This coincidence results in the amplification of the peak of the grid's electricity import cost and GHG emissions during the peak of these scenarios' net electricity demand, a phenomenon identified earlier in Emami et al., (2018). That is why the operating cost and GHG emissions need to be assessed along with the energy impact analysis in studies such as this.

Fig. 6 illustrates the overall annual total electricity demand breakdown for the main treatment units for each scenario.

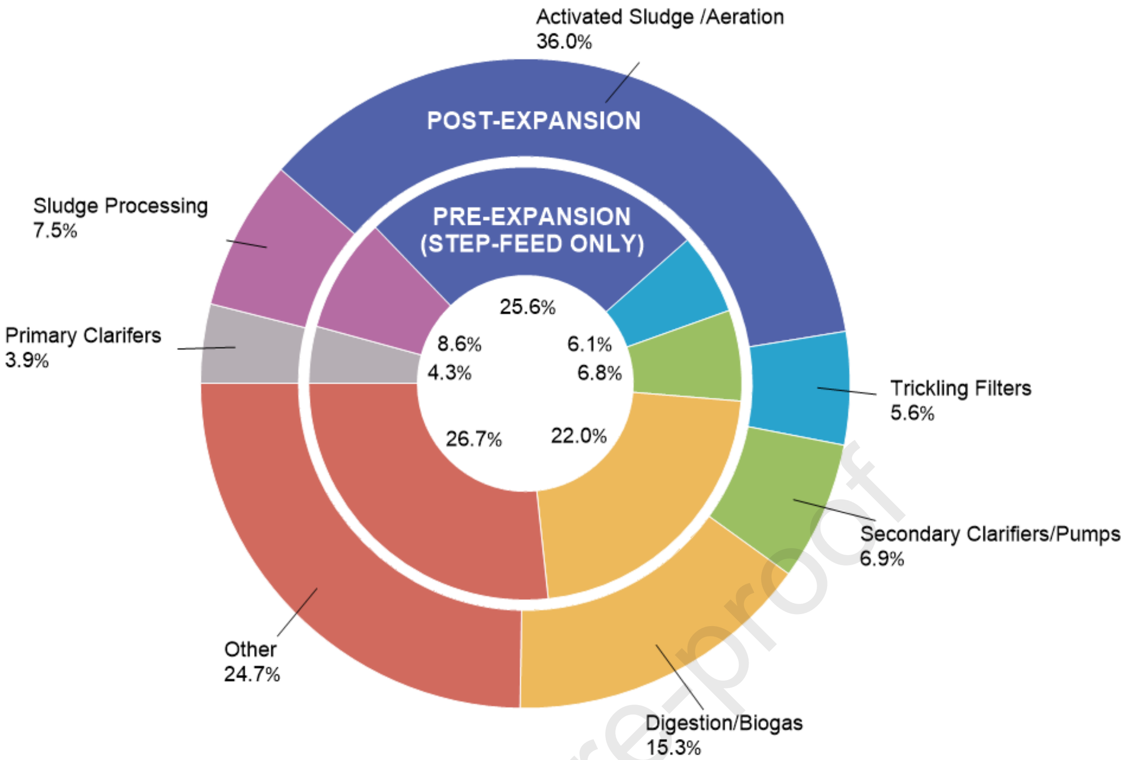

Fig. 6. Total electricity demand breakdown by process for the two scenarios. The total average daily electricity demand of post- and pre-expansion scenarios normalized to their influent flows are 0.53 kWh m^{-3} and 0.49 kWh m^{-3}, respectively.

The main difference in electricity demand breakdown for these two scenarios is in the activated sludge aeration electricity demand, and there is a larger proportion for the post-expnasion plant (i.e., 36.0% vs. 25.6%). This difference can be attributed to the different depth for the two processes, with the new expansion (AS2) being deeper (>7m, compared to the previous ~4.5m) and the consequent effect of this on the weighted sum of the two processes in the post-expansion configuration. Deeper tanks require more pressure from the blowers to support air discharge (Metcalf & Eddy, 2014), but have the associated limitation of lower floor area per unit tank volume. Hence, the diffusers installed there must be operated at higher air flux, which is inevitably linked to lower oxygen transfer efficiency (USEPA, 1989; Rosso et al, 2005). Since the total electricity demand of this scenario is higher than the pre-expansion plant's demand, this higher percentage represents a relevant increase in aeration electricity demand after the facility expansion. In other words, the addition of the new configuration has increased the plant's overall activated sludge electricity demand and so has not expanded its options for demand-side flexibility projects by providing a process change that saves electricity.

The only other category that shows an increase in electricity demand post expansion is secondary treatment pumping and clarifiers. This small increase is mainly due to additional pumping electricity associated with the AS2 MLE recycle stream in the expanded plant. This is a small contribution since, in this facility, the MLE pump of AS2 consumes less than 5% of the AS2 aeration energy. All other categories of the process energy demand breakdown show a small reduction after expansion.

The electrical energy intensity and demand breakdown comparison discussed here does not account for the improved treatment and effluent quality post expansion. Therefore, the effect of expansion on monthly electricity demand is reviewed further using other normalization options that account for this key element in the following sections.

3.3 Monthly Electricity Demand Comparison

The monthly electricity demands of these two scenarios are compared using the following three normalization methods that account for extent of treatment.

3.3.1 Activated Sludge Energy Intensity

Since the main difference between the two scenarios' electricity demand is driven by the secondary treatment process energy (dominated by aeration), the comparison in aeration electricity demand is highlighted here using activated sludge energy intensity in Fig.7.

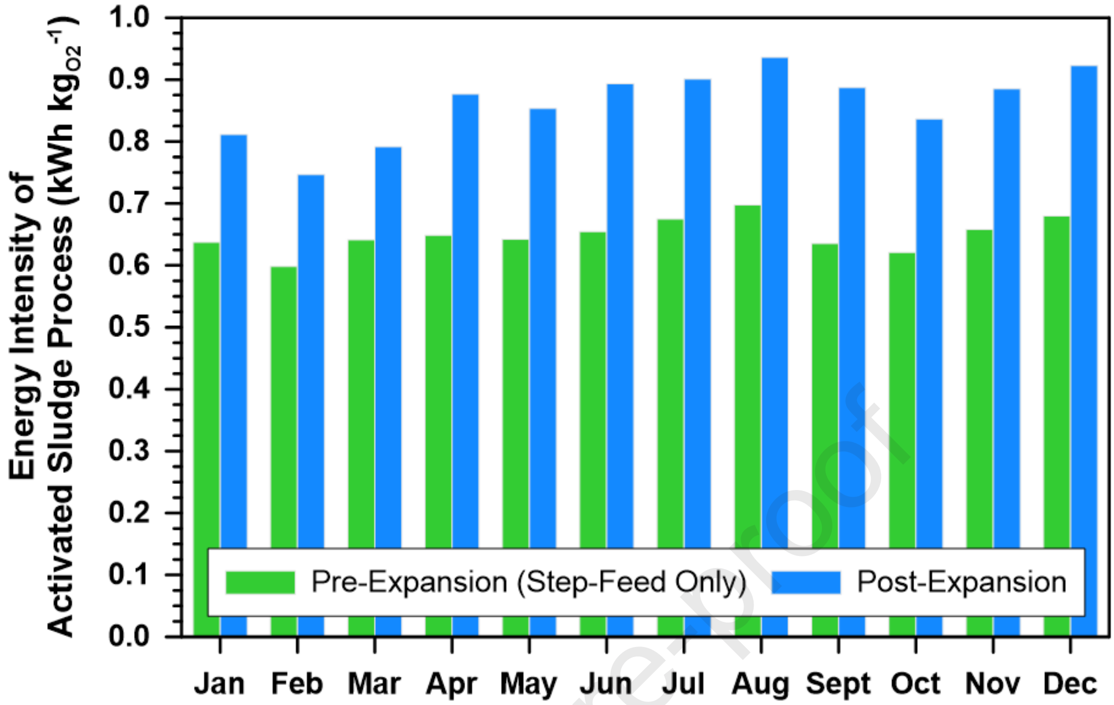

Fig. 7. Comparison of the activated sludge electrical energy intensity, defined as the electrical demand per unit of theoretical oxygen requirements.

As Fig. 7 illustrates, the activated sludge energy intensity of the post-expansion scenario is consistently higher than the pre-expansion's by approximately 33% on average. After accounting for the higher extent of removal in the post-expansion plant's activated sludge, it appears that in this scenario the activated sludge process is less energy-efficient. This conclusion is driven by the energy-intensity of the AS2 MLE activated sludge units added after expansion, which includes the MLE internal recirculation beside aeration and sludge return. This suggests the higher electricity efficiency of the step-feed L-E configuration comparing to MLE.

Since no alpha factors for the AS2 were available, the assumptions made for this basin's alpha were selected conservatively, which could have resulted in a conservative estimation of the electrical demand for AS2. Only a direct measurement of the alpha factors could verify these assumptions. Despite this seemingly higher energy intensity, the post-expansion scenario offers the benefits of increased nitrogen removal which contributes to the oxygen requirements in the normalization used in Fig.7, thus suggesting that alternate methods of normalization which are fair to the increased quality of the effluent water are needed. Additionally and more importantly, the plant reaches a now improved solids separation in secondary effluent, a characteristic of plants with longer sludge retention time (Chan et al, 2011; Li and Stenstrom, 2018). This benefit is welcomed by the downstream reuse operations, whose efficiency is marred by suspended solids (MWH, 2012). In addition, processes operating at longer sludge retention time are associated with improved removal of trace organics (Leu et al, 2010) which further enhances the quality of effluent water.

3.3.2 Electricity Demand to Quality Index Removal Ratio

Normalized net and total electricity demand for each scenario's quality index (Jeppsson, et al., 2007; Nopens, et al., 2010) removal for each month of the year are compared in Fig. 8.

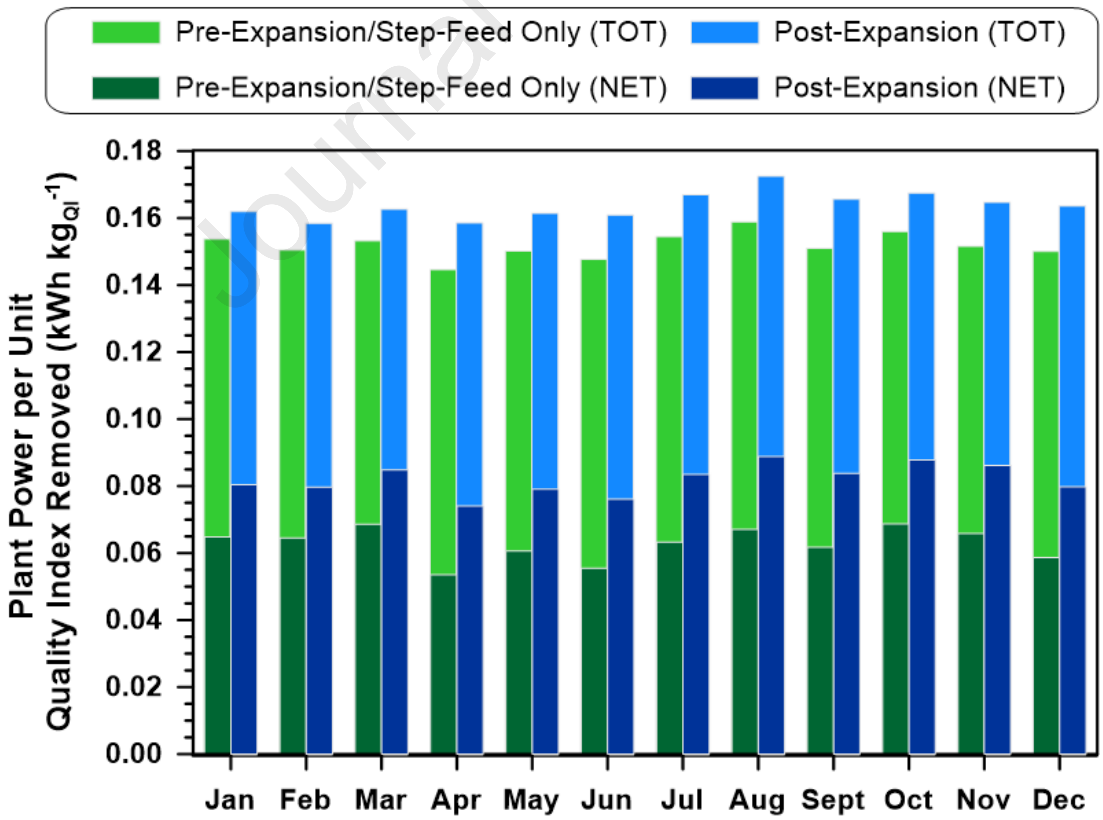

Fig. 8. Plant total and net electricity demand normalized per unit quality index removal, for both scenarios.

Fig. 8 demonstrates that both total and net electricity demand to QIR ratios are lower for the pre-expansion scenario by 5-9% and 19-28% of the post-expansion's, respectively. In other words, even after accounting for the plantwide higher cumulative extent of removal in the post-expansion scenario, it still requires more electrical energy for treatment. The extent of this electricity demand discrepancy doubles when net electricity demand is compared as illustrated in Fig. 8.

3.3.3 Electricity Demand to Oxidized Load Ratio

Fig. 9 compares the normalized net electricity demand to oxidized load for both scenarios without supplemental carbon addition.

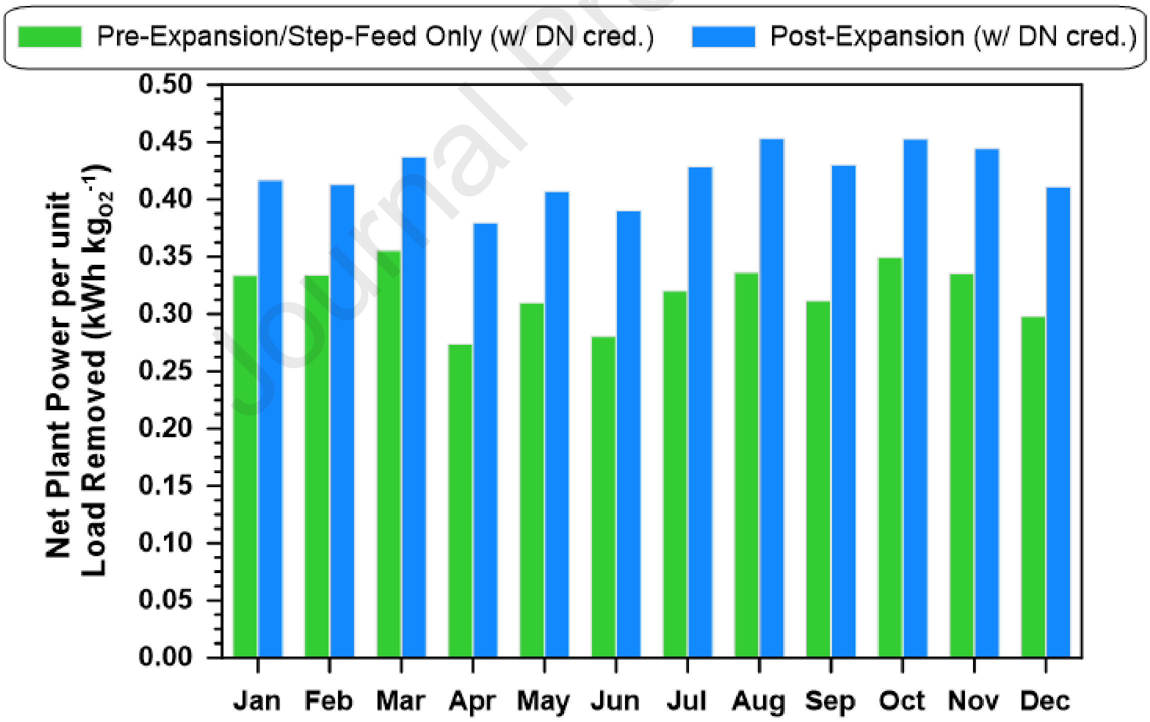

Fig. 9. Net electricity demand normalized per unit of total oxidized load for the two scenarios with denitrification credit (i.e., without supplemental carbon).

Similarly to the other electricity demand normalizations options, normalizing the net electricity demand per unit of oxidized load without supplemental carbon also confirms that the pre-expansion scenario is the more energy-efficient option by 19-28%.

In summary, all the normalization methods used to compare these scenarios electricity demand concludes that the expanded plant is less electricity efficient which translates into demonstrating the MLE configuration as less electricity efficient compared to the step-feed L-E in this facility. We attribute this difference to the depth of the MLE process, which places the operating point and efficiency of the aeration diffusers at a disadvantage compared to the L-E process. In addition, the current MLE recycle stream flow is another suspect for this lower efficiency which is recommended for further evaluation in future studies. More details on this observation have been provided in the Recommendations and Future Research section of this paper.

3.4 Greenhouse Gas Emissions

The average daily GHG emissions breakdown by source types are compared in Fig. 10. The major sources of GHG emissions are the activated sludge and digester processes which consist of CO_2, CH_4, and N_2O emissions generated by activated sludge and CO_2 emission generated by the digester. The combustion emissions (biogas and natural gas), consist of CO_2, CH_4, and N_2O emissions, constitute the second major source of emissions followed by electricity import CO_2 and fugitive leak (CH_4) emissions.

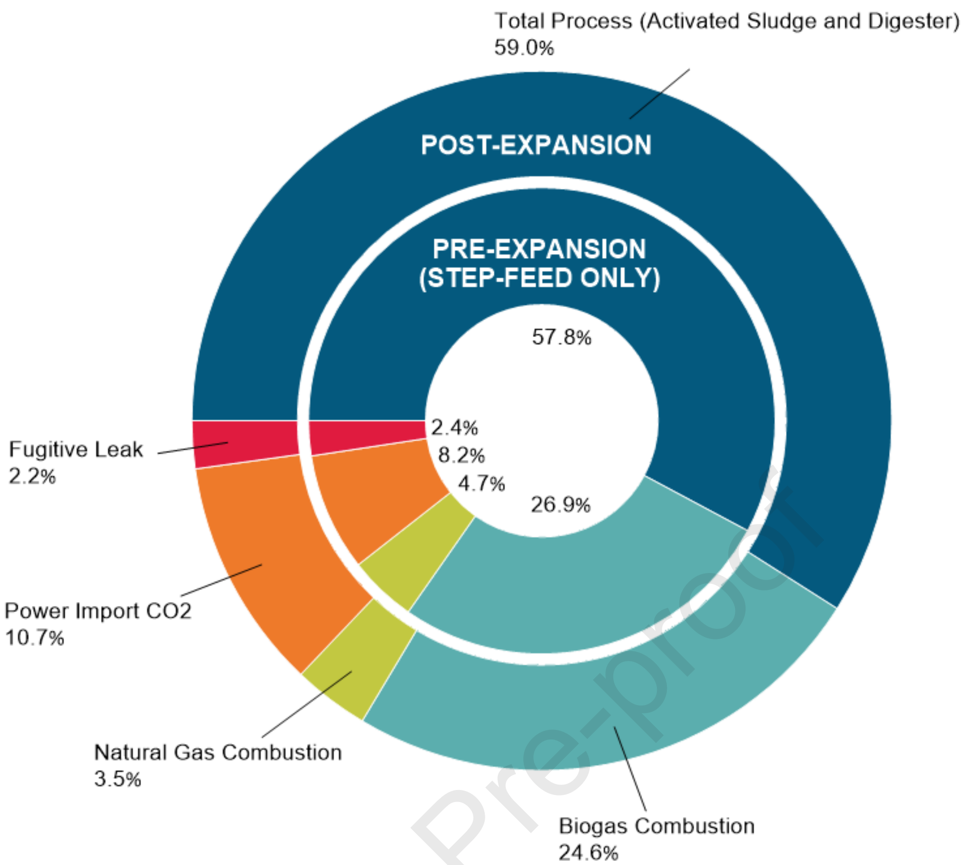

Fig. 10. Greenhouse gas emissions breakdown by source type for both scenarios. The total average daily emissions per unit influent flow treated for post- and pre- expansion scenarios are really close (0.623 $kgCO_2eq\ m^{-3}$ and 0.619 $kgCO_2eq\ m^{-3}$, respectively).

The biogas fugitive leak emissions calculated here are heavily reliant on the assumption used as there are no direct measurements of the fugitive digester gas, and biogas flow metering is not sufficiently accurate to quantify these. Therefore, its emission quantification has not been captured in GHG quantification protocols (Willis et al., 2016). The margin of accuracy of the flow meters also makes the quantification of biogas fugitive emissions using mass or flow balance from field data very difficult if not impossible. The fugitive emission assumption of 1.0% of the total biogas production implemented in this study can easily fall in the range of accuracy of the typical flowmeters capable of reading gas flows at a wastewater treatment plant, ranging from 0.5 to 2.0% (U.S. EPA Region 4, 2020). Previously, the assumption of 2% was used in several studies (*inter alia*, Gori et al., 2011; Gori et al., 2013) since it was within the typical margin of error for most large-scale biogas flow meters (i.e., >5%) and corresponded to the assumption by Monteith et al., (2005). Nevertheless, this range of assumptions has been highlighted as a knowledge gap as early as 2008 (Foley and Lant, 2008) and has yet to be fully addressed. A sensitivity analysis was performed to demonstrate the effect of increasing fugitive emissions from 1% to 15% on the plant's overall GHG breakdown for these two scenarios (Fig. H.1 in Appendix H). Incrementally accounting for fugitive emission results in almost doubling its overall emissions contribution in this sensitivity analysis (2% to 25% in this study) due to methane's global warming potential of 25 (U.S. EPA, 2014).

A comparison of monthly GHG emissions normalized to QIR for these scenarios, calculated to account for the overall extent of treatment, also demonstrates a small difference (± 2%) between these scenarios. It also illustrates a subtle seasonality with the post-expansion scenario having slightly lower emissions in the colder months (October through April). More details have been provided in Appendix I.

3.5 Operating Cost Ratio

For both scenarios, the operating cost based on the 5 different electricity tariff structures presented in Fig. 4 were compared. In addition to the grid's electricity cost, we considered the cost of: chemicals used for enhancing primary treatment; sludge dewatering and thickening chemical additives; biosolid disposal; and natural gas imports. The costs are normalized per unit QIR to also account for the extent of the treatment. Since each treatment scenario would have 5 tariff sub-scenarios, the ratio of the normalized total operating cost of the post-expansion scenario to the pre-expansion's for each power tariff is summarised in Fig. 11 to simplify the comparison.

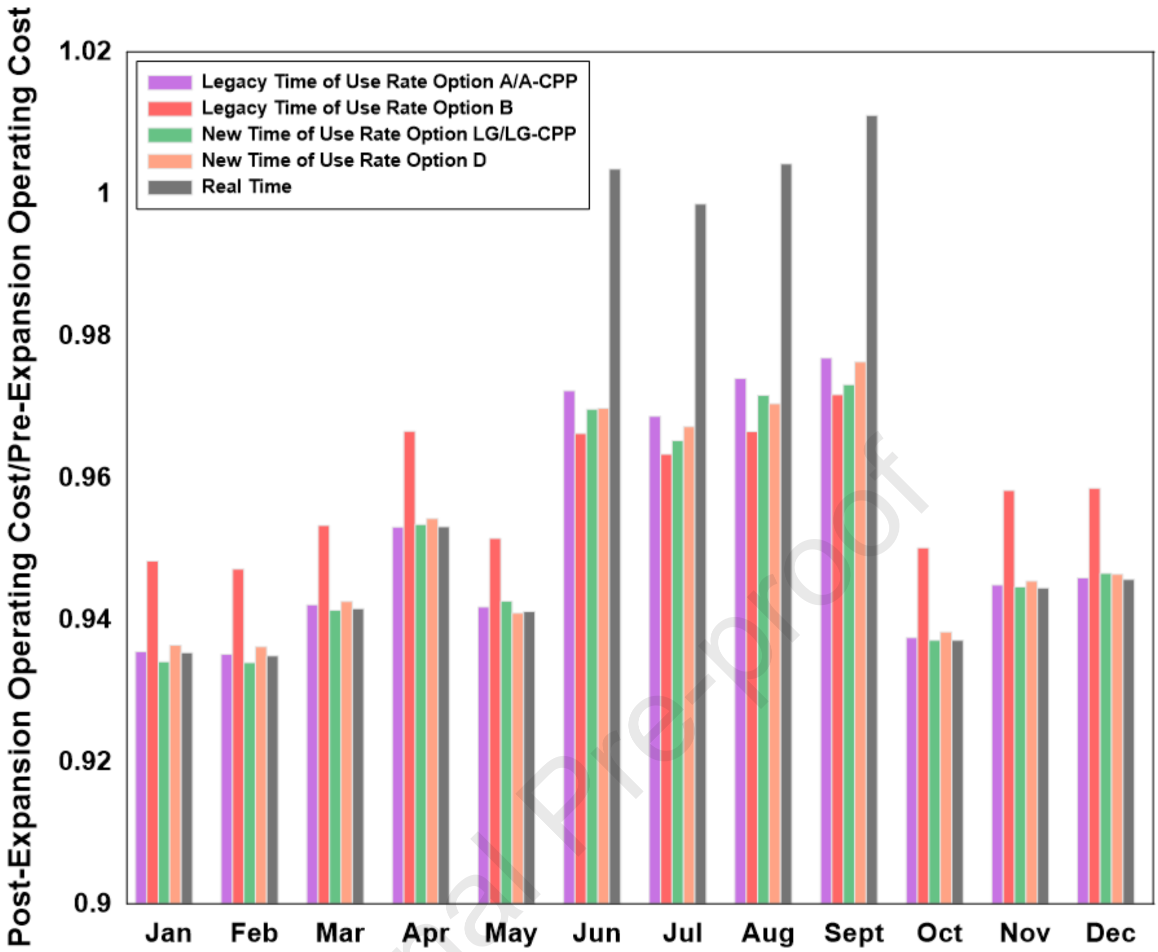

Fig. 11. Operating cost per unit quality index removal for both scenarios, applying the five power tariffs in Fig.4 and their calculated average. The results are presented as dimensionless ratios, with the pre-expansion scenario in the denominator. Annual operating cost to unit quality index removal ratio calculated using the average of these 5 tariffs annual electricity cost for post- and pre-expansion scenarios are 41.98 USD per metric ton and 43.90 USD per metric ton respectively.

According to Fig. 11, the operating cost calculated using all five electricity tariffs for this plant have been reduced post expansion for every month except for the Real Time tariff in summer months when the cost is almost the same or about 1% higher. As shown in Fig. 11, tariff options B (a legacy tariff) and Real Time (a new tariff) resulted in a more significant difference among these five tariffs in winter and summer months respectively. This demonstrates the significant effect of different tariff structures on the economic outcome of a modification and why changes in the electricity tariff structure in response to the increase of renewable electricity sources, captured in new tariff (e.g., Real Time), can significantly impact WRRFs operating cost.

The significantly higher operating cost of the Real Time option in the summer compared to the other tariffs can be explained by its significantly higher summer energy usage charges during peak demand periods when compared to all other tariffs. The higher cost of Option B in the winter months can be explained by having the highest excess capacity reserve charge component of the facility electricity demand charge among all power tariffs. This charge applies to the portion of the facility total electricity demand that exceeds a standby demand agreed upon between the facility and the electricity provider. This standby demand was assumed to be the same as the typical facility average electricity generation nameplate capacity for this study (i.e., 5.2 MW as explained in the Methods section). More details about the demand charges for each of these tariffs are provided in Appendix J. Although this higher facility demand charge for Option B should have impacted all the months of the year and not only winter, this option’s lower total energy usage charges in the summer compared to the winter, which is unique to this tariff option, have alleviated its high demand charge in the summer months.

Fig. 11 also clearly demonstrates the seasonality of electricity cost and how the higher cost of electricity in summer months can significantly increase the operating cost of the WRRF. All the tariff sub-scenarios show significantly higher operating cost difference for these two operating scenarios in the summer months, which can be explained by the higher electricity cost (i.e., total energy usage or demand charges) especially during the peak of electricity demand as reported in Fig. 4 and Appendix J. This is also another factor that proves the importance of applying the dynamic power tariff profiles in the accuracy of modelling efforts such as this one as opposed to an average value for the entire year which ignores this significant cost increase.

The overall lower operating cost of the post-expansion scenario illustrated by ratios <1 in Fig. 11 for almost all the tariffs demonstrates that the non-electricity portion of operating cost components accounted for in this study compensates this scenario’s slightly higher electricity cost. Comparing the other annual operating cost components values normalized to the QIR suggests that these compensating components are chemical and natural gas usage cost with the chemical usage being the dominant cost. Since the primary treatment has not been impacted by the expansion project, the chemical usage for enhancing its performance and thickening and dewatering its sludge after being normalized to total QIR is expected to be comparable for both scenarios. Therefore, the chemical usage cost savings is narrowed down to be of the secondary treatment's waste sludge dewatering and thickening. The lower normalized secondary sludge waste stream flow that goes through dewatering and thickening in the post-expansion scenario compared to the pre-expansion's clearly explains the chemical usage cost savings of this option which is calculated from this stream flowrate using a constant cost to flow ratio. This lower secondary sludge waste generation can be explained by better solids separation in secondary treatment of the expanded plant as a result of its activated sludge longer sludge retention time in the MLE reactors (Chan et al, 2011; Li and Stenstrom, 2018).

In addition to less chemical demand, post-expansion scenario's lower sludge waste production reduces its thermal energy demand at the facility digesters and increases the digesters' capacity (i.e., their retention time). This results in reducing this scenario's natural gas import by lowering its overall thermal energy demand and increasing its biogas production, which is largely driven by primary sludge conversion to methane (Gori et al, 2013). This phenomenon can be clearly demonstrated by the lower normalized natural gas usage cost to QIR in the post-expansion scenario compared to the pre-expansion's.

In sum, the expansion of the plant had other benefits than just increasing the facility treatment capacity. These additional benefits included improvement of the overall effluent quality of the facility as well as reducing its natural gas and chemical demands which results in the overall reduction of the treatment cost and ultimately of its environmental footprint. This overall operating cost reduction demonstrates that the combined chemical and natural gas demands cost savings of the expansion overcomes its electricity cost increase and that the less electricity efficient combination of the AS configurations post-expansion is more cost effective. In other words, lowering the plant electricity demand by increasing the use of more electricity efficient activated sludge configuration (AS1) results in increasing the overall operating cost and effluent pollution which makes such an electricity saving undesirable and infeasible for this WRRF.

This inverse effect of reducing this facility's electricity demand by increasing the use of its more electricity efficient activated sludge configuration of the two on its overall operating cost demonstrates the infeasibly of the proposed demand-side flexibility project in the Introduction section of this article. This conclusion and inverse effect, however, can be reversed by increasing the electricity efficiency of the MLE configuration to exceed the Step-feed's. In this case, the electricity cost savings associated with increasing the use of more efficient configuration (MLE) is added to this configuration's chemical and natural gas demand cost savings. Thus, this electricity saving project becomes economically feasible and in fact desirable from the facility management point of view. This electricity savings also lowers the plant's overall carbon footprint by lowering the contribution of the indirect greenhouse gas emissions associated with the imported electricity from the grid.

3.6 Recommendations and Future Research

Data collection and validation were the most challenging phase of this study and required years of expert investigative work. One of the challenging factors in data collection was the low frequency of data collection and recording (mostly monthly). Additionally, the patchwork of data acquisition and storage systems, typical of large facilities that underwent a succession of upgrades and expansions, increases the challenge of accessing data. A higher frequency of data sampling and recording that at least represents the on- and off- diurnal influent peaks is recommended to be performed by WRRFs for future studies. This not only results in more accurate dynamic modelling results, but also simplifies data validation and actions to address missing data.

In this modelling effort, not all influent fractions could be derived from field data collected by the plant (e.g., NH_3/TKN). As such, we recommend additional sampling to derive these ratios before starting the modelling effort in the future. The accuracy of the flow data used for modelling and validating the simulation of different process units is crucial. Calibrating and operating the flowmeters according to manufacturers' guidelines by the facility as well as using the data from such meters, when available, are strongly recommended here. Also, a lack of dynamic electricity demand data broken down to major process units, which is necessary for developing a complete dynamic facility electricity demand model, was another challenge that had to be confronted here. Equipment models can assist in this task.

By comparing the effluent nitrogen (ammonia, nitrite, and nitrate) trends with the plant's influent ammonia (~66% of influent TKN-N; Appendix F), we concluded slightly higher nitrification and denitrification in the post-expansion scenario. This is despite the fact that much higher denitrification and lower effluent nitrate and ammonia concentrations are expected from this scenario after the addition of MLE. This lower denitrification performance is likely due to high MLE recycle-stream flow and is a potential explanation for higher aeration electricity demand post-expansion. Thus, further studies to investigate this issue are also recommended for the plant studied here in addition to collecting field alpha data for the MLE configuration as noted above.

The MLE recycle stream at the expanded plant is set at about 200% of the AS2 influent. High flow recycle streams in the AS2 bioreactors in series results in a deviation of the performance of these reactors from plug-flow to continuous stirred tank reactor (CSTR) configuration which is characterized by lower conversion rates. Therefore, the extent of denitrification may have been lowered by excessive MLE internal recycling here. The effect of lowering this recycle stream flow on the normalized results would be twofold: reduction of pumping energy and increased plug-flow characteristics (hence, higher pollutant removal in the same reactor volume).

3.7 Limitations and Considerations

The results of this study should not be blindly extended to other plants. Each plant has its own characteristics, treatment targets, and distinct geometry and equipment. In this facility, the concentration of nitrogen in the effluent is almost immaterial and effluent solids concentration is the main treatment concern. Thus, optimizing the nitrogen in effluent is a minor priority as opposed to other plants where water reclamation results in distribution (e.g., for irrigation). In extrapolating the results of activated sludge basins in this study to other plants with similar volumes, the geometry must also be accounted for. The reduced length deviates this reactor from plug-flow configuration and makes it more like a CSTR at the cost of lowering the extent of reaction and removal. Additionally, for a given volume, reactors with reduced surface area must be deeper, which reduces the number of diffusers that can be installed on the tank floor and forces their operating point at higher flux (i.e., less efficient). Analysing the geometry on a case-specific basis and optimizing the flow rate for returns to make sure the denitrification meets the target of that specific utility is more important than trying to infer that the findings here are true for every plant with the same process volumes. Similarly, site-specific dynamic electricity tariffs, power grid GHG intensities, and alpha factors need to be considered before extending the results of this study to other plants.

4 SUMMARY AND CONCLUSIONS

This article underscored how the diurnal cycles and peaks of the grid electricity tariffs and carbon intensity coincide with a large WRRF's peak of influent load and electricity demand in California. Illustrating the coincidence of these parameters and the amplifying effect of this coincidence in the facility electricity import cost and carbon footprint substantiates the importance of dynamic modelling for these facilities to correctly assess their electricity demand cost and carbon footprint.

A coupled bioprocess and electricity dynamic analysis was performed to study the effect of an expansion project on electricity demand, carbon footprint, and the operating cost of this facility. This facility was selected because it has two independent parallel activated sludge process configurations after this expansion which are fed the same influent. This parallel set up facilitates the reduction of the expanded facility's overall electricity demand by increasing the more electricity efficient configuration's share of the influent treatment. The coincidence of this plant's peak of electricity demand with the power grid's peak of cost and carbon intensity suggests an additional benefit for this potential electricity-saving option during the grid's peak of demand which can be a target for demand-side flexibility incentives.

Comparing both the net and total electricity demand of this WRRF for pre- and post-expansion scenarios and accounting for these scenarios' extent of treatment using different normalization methods demonstrated that the addition of the second activated sludge configuration (MLE) has decreased the activated sludge and plant's overall electricity efficiency. However, this addition was determined to reduce the plant's operating cost (despite the increase in its electricity demand and cost) and slightly improve its effluent quality without a significant impact on its carbon footprint. These findings demonstrate how an increase in energy intensity is ultimately compensated by a decrease in overall operating cost due to the change in chemicals and natural gas usages in the new configuration. This inverse correlation between electricity demand and overall operating cost of the expanded plant also substantiates the infeasibility of the demand-side flexibility project that targets electricity savings by maximizing the use of the more energy efficient activated sludge configuration in this plant.

By lowering the plant's overall activated sludge energy efficiency, despite the expectation for having a higher energy efficiency than the existing activated sludge configuration (step-feed L-E), the added configuration (MLE) post-expansion demonstrates a need for optimization and further analysis of the process geometry as it relates to its energy intensity. The MLE recycle stream flow adjustment is an area that this study suggests as a target for such process optimization efforts in future studies. Such an optimization is expected to also improve the effluent quality in addition to other cost and carbon footprint reductions associated with electricity savings resulting from this optimization. In addition, such an optimization project can reverse the conclusion of this study on the feasibility of the demand-side flexibility project that maximizes the use of the more energy efficient activated sludge configuration in this facility if the optimized MLE configuration exceeds the energy efficiency of step-feed L-E's.

To repeat the same modelling effort in the future, this study also recommends increasing the frequency of field data collection along with collecting additional field data that were not available here. These additional field data include but are not limited to: alpha values for Activated Sludge 2, electricity demand data by process units, influent ammonia to TKN ratio, and effluent nitrate and nitrite concentrations. Caution must be exercised when generalizing the results of this study to other WRRFs, because these results should not be assumed without accounting for those plants' characteristics, treatment goals, and distinct geometry differences as well as their site-specific dynamic grid electricity tariffs, GHG intensities, and alpha factors.

CRediT Authorship Contribution Statement

Mani Firouzian: Conceptualization; Data compilation; Data curation; Modelling; Formal analysis; Investigation; Methodology; Visualization; Writing original draft; Writing review & editing.

Michael K. Stenstrom: Experimental work; Writing review & editing.

Diego Rosso: Supervision; Conceptualization; Research design; Experimental work; Visualization; Writing review & editing.

Funding

This research did not receive any specific grant from funding agencies in the public, commercial, or not-for-profit sectors.

Acknowledgments

The authors thank the utility personnel who supplied data and information.

REFERENCES

American Society of Civil Engineers. (2018). ASCE Standard ASCE/EWRI 18-18. In Standard Guidelines for In-Process Oxygen Transfer Testing. Reston, VA: American Society of Civil Engineers.Amerlinck, Y., De Keyser, W., Urchegui, G., & Nopens, I. (2016). A realistic dynamic blower energy consumption model for wastewater applications. *Water Science & Technology, 74*(7), 1561–1576. doi:10.2166/wst.2016.360

Amerlinck, Y., De Keyser, W., Urchegui, G., Nopens, I., 2016. A realistic dynamic blower energy consumption model for wastewater applications. Water Science & Technology 74 (7), 1561–1576. DOI: 10.2166/wst.2016.360

Aymerich, I., Rieger, L., Sobhani, R., Rosso, D., & Corominas, L. (2015). The difference between energy consumption and energy cost: Modelling energy tariff structures for water resource recovery facilities. *Water Research, 81*, 113-123. doi:10.1016/j.watres.2015.04.033

Baird, R., Eaton, A. D., Rice, E. W., & Bridgewater, L. (2017). *Standard Methods for the Examination of Water and Wastewater / prepared and published jointly by American Public Health Association, American Water Works Association, Water Environment Federation ; joint editorial board, Rodger B. Baird, Andrew D. Eaton, Eugene W. Rice ; managing editor, Laura Bridgewater.* (Twenty-third edition.). American Public Health Association.

California Independent System Operator. Today's Outlook. Retrieved from California Independent System Operator: http://www.caiso.com/TodaysOutlook/Pages/index.html (last accessed on 2021, 05 22)

Caliskaner, O., Tchobanoglous, G., Reid, T., Davis, B., Young, R., & Downey, M. (2017). First Full-Scale Installation of Primary Filtration for Advanced Primary Treatment to Save Energy and Increased Capacity. Proceedings of the 2017 Water Environment Federation Technical Exhibition and Conference. New Orleans, Louisiana: Water Environment Federation.

Caliskaner, O., Tchobanoglous, G., Reid, T., Young, R., Downey, M., & Kunzman, B. (2016). Advanced Primary Treatment via Filtration to Increase Energy Savings and Plant Capacity. Proceedings of the 89th Annual Water Environment Federation Technical Exposition and Conference. New Orleans, Louisiana: Water Environment Federation.

Caliskaner, O., Tchobanoglous, G., Wu, Z., Young, R., Paez, C., Davis, B., Mansell, B., Ackman, P., Reid, T., & Dyson, J. (2018). Performance of Full Scale and Demonstration-Scale Primary Filtration Projects. Proceedings of the 2018 Water Environment Federation Technical Exhibition and Conference (pp. 70-84). New Orleans, Louisiana: Water Environment Federation.

Chan, L., Leu, S.-Y., Rosso, D., & Stenstrom, M.K. (2011). The Relationship Between Mixed-Liquor Particle Size and Solids Retention Time in the Activated Sludge Process. *Water Environment Research, 83*(12), 2178-2186. doi:10.2175/106143011X12928814445339

Christian, R. (2018, 9 10). What California’s 100% clean energy mandate means for the United States. PV magazine USA.

Emami, N., Sobhani, R., & Rosso, D. (2018). Diurnal variations of the energy intensity and associated greenhouse gas emissions for activated sludge processes. *Water Science and Technology, 77*(7), 1838-1850. doi:10.2166/wst.2018.054

EnviroSim. (2020). BioWin 6.1 Help Manual. Hamilton, Ontario: EnviroSim.

Foley, J., & Lant, P. (2008). *Fugitive Greenhouse Gas Emissions from Wastewater Systems: WSAA Literature Review No.01*. Water Services Association of Australia, Melbourne.

Gonzalez-Salazar, M. A., Prchlik, L., & Kirsten, T. (2018). Review of the operational flexibility and emissions of gas- and coal-fired power plants in a future with growing renewables. Renewable Sustainable Energy, 82, 1497-1513. doi:10.1016/j.rser.2017.05.278

Gori, R., Giaccherini, F., Jiang, L., Sobhani, R., & Rosso, D. (2013). Role of primary sedimentation on plant-wide energy recovery and carbon footprint. Water Science & Technology, 68(4), 870-878. doi:10.2166/wst.2013.270

Gori, R., Jiang, L., Sobhani, R., & Rosso, D. (2011). Effects of soluble and particulate substrate on the carbon and energy footprint of wastewater treatment processes. Water Research(45), 5858-5872. doi:10.1016/j.watres.2011.08.036

Howlader, H. O. R., Sediqi, M. M., Ibrahimi, A. M., & Senjyu, T. (2018). Optimal Thermal Unit Commitment for Solving Duck Curve Problem by Introducing CSP, PSH and Demand Response. IEEE Access, 6, 4834-4844. doi:10.1109/ACCESS.2018.2790967

Howlader, H. O., Furukakoi, M., Matayoshi, H., & Senjyu, T. (2017). Duck Curve Problem Solving Strategies with Thermal Unit Commitment by Introducing Pumped Storage Hydroelectricity & Renewable Energy. 2017 IEEE 12th International Conference on Power Electronics and Drive Systems (PEDS) (pp. 502-506). Honolulu, HI, 2017, pp.: IEEE.

Jeppsson, U., Pons, M.-N., Nopens, I., Alex, J., Copp, J.B., Gernaey, K.V., Rosen, C., Steyer, J.-P., &Vanrolleghem, P.A. (2007). Benchmark simulation model no 2: general protocol and exploratory case studies. Water Science & Technology, 56(8), 67-78. doi:10.2166/wst.2007.604

Jiang, L. M., Garrido-Baserba, M., Nolasco, D., Al-Omari, A., DeClippeleir, H., Murthy, S., & Rosso, D. (2017). Modelling oxygen transfer using dynamic alpha factors. Water Research, 124, 139-148. doi:10.1016/j.watres.2017.07.032

Leu, S.-Y., Chan. L., & Stenstrom, M.K. (2010) Toward Long SRT of Activated Sludge Processes: Benefits in Energy Saving, Effluent Quality, and Stability, *Wat. Environ. Res*., 8, 7282-7295

Li, Z., & Stenstrom, M.K. (2018). Impacts of SRT on Particle Size Distribution and Reactor Performance in Activated Sludge Processes. Water Environment Research, 90(1), 48-56. doi:10.2175/106143017X15054988926523

Metcalf, & Eddy. (2014). *Wastewater Engineering: Treatment and Resource Recovery* (5^{th} ed.). New York: McGraw-Hill Education.

Monteith, H.D., Sahely, H.R., MacLean, H.L., & Bagley, D.B. (2005). A rational procedure for estimation of greenhouse-gas emissions from municipal wastewater treatment plants. *Water Environment Research, 77*(4), 390-403. doi:10.2175/106143005X51978

Musabandesu, E., & Loge, F. (2021). Load shifting at wastewater treatment plants: A case study for participating as an energy demand resource. *Journal of Cleaner Prodcution, 282*. doi:10.1016/j.jclepro.2020.124454

MWH. (2012). *Water Treatment: Principles and Design* (2nd ed.). Hoboken, NJ: John Wiley & Sons.

Nopens, I., Benedetti, L., Jeppsson, U., Pons, M.-N., Alex, J., Copp, J. B., Gernaey, K. V., Rosen, C., Steyer, J.-P., & Vanrolleghem, P. A. (2010). Benchmark Simulation Model No 2: finalisation of plant layout and default control strategy. Water Science & Technology, 62(9), 1967-1974. doi:10.2166/wst.2010.044

Olsson, G. (2015). *Water and Energy: Threats and Opportunities* (2nd ed.). London, UK: IWA Publishing.

Pabi, S., Amarnath, A., Goldstein, R., & Reekie, L. (2013). Electricity Use and Management in the Municipal Water Supply and Wastewater Industries. Palo Alto, California: Electric Power Research Institute & Water Research Foundation.

Panepinto, D., Fiore, S., Zappone, M., Genon, G., & Meucci, L. (2016). Evaluation of the energy efficiency of a large wastewater treatment plant in Italy. *Applied Energy, 161*, 404-411. doi:10.1016/j.apenergy.2015.10.027

Pasini, F., Garrido-Baserba, M., Ahmed, A., Nakhla, G., Santoro, D., & Rosso, D. (2020). Oxygen transfer and wide-plant energy assessment of primary screening in WRRFs. Water Environment Research, 1-16. doi:10.1002/wer.1349

Reardon, D. (1995). Turning down the power. Civil Engineering, 65(8), 54-56.

Rieger, L., Gillot, S., Langergraber, G., Ohtsuki, T., Shaw, A., Takacs, I., & Winkler, S. (2013). Guidelines for Using Activated Sludge Models. London: IWA.

Rosso, D., Iranpour, R., Stenstrom, M.K. (2005). Fifteen years of OTE measurements on fine-pore aerators: key role of sludge age and normalized air flux, *Wat. Env. Res.*, 77, 266-273.

Rosso, D., & Stenstrom, M.K. (2007). Energy-saving benefits of denitrification. *Environmental Engineering, 43*(3), 29-38.

Schäfer, M., Hobus, I., & Schmitt, T.G. (2017). Energetic flexibility on wastewater treatment plants. *Water Science and Technology, 76*(5), 1225-1233. doi:10.2166/wst.2017.308

Sobhani, R., Jiang, L.-M., Chau, A., Brown, J., Torres, E., Shao, Y., & Rosso, D. (2011). Energy Footprint Analysis of Orange County Sanitation District's Operations. Water Environment Federation (pp. 3707-3714). Los Angeles: Water Environment Federation.

Southern California Edison. *SCE - Document Library*. Retrieved from Southern California Edison: https://library.sce.com/?10000_group.propertyvalues.property=jcr%3Acontent%2Fmetadata%2Fcq%3Atags&10000_group.propertyvalues.operation=equals&10000_group.propertyvalu

es.0_values=sce-document-library%3Aregulatory%2Fsce-tariff-books%2Felectric%2Fschedules%2 (last accessed on 2021, 05 22)

U.S.E.P.A. (1989). *Fine Pore Aeration Systems*. EPA/625/1-89/023.

U.S. EPA. (2014, 12 11). Title 40 Part 98—Mandatory Greenhouse Gas Reporting-Subpart A—General Provision. Retrieved from Electronic Code of Federal Regulations: https://www.ecfr.gov/cgi-bin/text-idx?SID=c928f22246db4fd098e7ed7cdf75a869&mc=true&node=pt40.23.98&rgn=div5#sp40.23.98.a (last accessed on 2021, 05 22)

U.S. EPA. (2016, 09 12). Title 40 Part 98—Mandatory Greenhouse Gas Reporting-Subpart C—General Stationary Fuel Combustion Sources. Retrieved from Electronic Code of Federal Regulations:https://www.ecfr.gov/cgi-bin/text-idx?SID=c928f22246db4fd098e7ed7cdf75a869&mc=true&node=pt40.23.98&rgn=div5#sp40.23.98.c (last accessed on 2021, 05 22)

U.S. EPA Region 4 Laboratory Services and Applied Sciences Division. (2020, 06 11). Wastewater Flow Measurement Operating Procedure. Wastewater Flow Measurement. Athens, Georgia. U.S.

Weather Underground. (2021). John Wayne Airport Station. Retrieved from Weather Underground: https://www.wunderground.com/history/monthly/us/ca/santa-ana/KSNA/date/2018-10 (last accessed on 2021, 05 22)

Willis, J., Yuan, Z., & Murthy, S. (2016). Wastewater GHG Accounting Protocols as Compared to the State of GHG Science. Water Environment Research, 88(8), 704-714. doi:10.2175/106143016X14609975746965

Declaration of interests

☒ The authors declare that they have no known competing financial interests or personal relationships that could have appeared to influence the work reported in this paper.

☐The authors declare the following financial interests/personal relationships which may be considered as potential competing interests: